Solving the Power Flow problem on Integrated Transmission-Distribution Networks: A Review and Numerical Assessment

Kootte, M.E.; Romate, Johan; Vuik, C.

Publication date
2021

Document Version
Final published version

Citation (APA)
Kootte, M. E., Romate, J., & Vuik, C. (2021). *Solving the Power Flow problem on Integrated Transmission-Distribution Networks: A Review and Numerical Assessment*. (Reports of the Delft Institute of Applied Mathematics; Vol. 21-01). Delft University of Technology.

DELFT UNIVERSITY OF TECHNOLOGY

REPORT 21-01

Solving the Power Flow problem on Integrated Transmission-Distribution Networks: A Review and Numerical Assessment

M.E. Kootte, J.E. Romate, and C. Vuik

ISSN 1389-6520

Reports of the Delft Institute of Applied Mathematics

Delft 2021

Solving the Power Flow problem on Integrated Transmission-Distribution Networks: A Review and Numerical Assessment

M.E. Kootte, J.E. Romate, C. Vuik

January 19, 2021

Abstract

Power flow simulations form an essential tool for electricity network analysis but conventional models are designed to work on a separated transmission or distribution network only. The continuing growth of electricity consumption, demand side participation, and renewable resources makes the electricity networks co-dependent. Integrated models incorporate the coupling of the networks and interaction that they have on each other, representing the power flow within this changing environment accurately.
Several numerical methods are available to solve the power flow problem on integrated networks. They can be categorized as a unified or as a splitting method and networks can be modeled as a homogeneous or hybrid network. In this paper, we review and assess these methods on the network models by running simulations on small test networks and comparing the outcome on their numerical performance, ie on convergence rate and CPU-time. The review shows that the convergence rate is comparable for most of the methods, but that hybrid networks have a slight advantage in computational time. Realistic network models, running on millions of buses and with large distribution networks, should give a better insight into the speed of the computations.

1 Introduction

Power flow computations are used to simulate the transport, generation, and consumption of power in electricity networks. The simulations are important for safe operation and planning of the electricity grid [1]. A national electricity grid consists of one transmission network, responsible for transport of power over large distances, and several distribution networks, responsible for the transport to end-consumers. Transmission networks transport high-voltage power to substations from where power is converted to a lower voltage level. The distribution network transports low-voltage power from substations to end-consumers. These transmission and distribution domains are currently separately analyzed: In the analysis of the first, the transmission network is modeled in detail while the distribution network is modeled as an equivalent load. In the analysis of the distribution system, this

system is modeled in detail while the transmission network is simplified as a power supply source.

The power system is changing: 1) more renewable energy is entering the grid at distribution level, 2) we see an increase of demand-side participation as a mechanism to balance frequency, and 3) we see an increase of electricity consumption [2]. The changing environment requires a more detailed analysis of the electricity network and a more complex model of the interaction between the networks. Integrated transmission-distribution network models study the interaction that these networks have on each other. But it is not straight-forward to integrate these separate domains. The networks have different characteristics what has resulted in different network models that cannot be easily integrated. The most important difference is that the transmission network is a balanced network: Power is generated in three phases but voltage and current of other phases have the same magnitude and are equally shifted in phase by $2/3\pi$ rad. Therefore, the transmission network is modeled in single-phase while the distribution network is in general not balanced and thus modeled in three-phase [3]. Furthermore, the different characteristics have lead to the development of different algorithms to solve the power flow problem of different systems. The power flow problem is a nonlinear problem which is solved using iterative methods. Well-known algorithms to solve transmission systems are: Gauss-Seidel, Newton-Raphson, Decoupled loadflow, and DC loadflow [4]. These solvers have been adapted to distribution solvers, among which the most well-known are: Newton-Raphson current mismatch [5] [6], implicit Z_{bus} [7] [8], BIBC/BCBV [9] [10], and Forward/Backward Sweep [11] [12] methods.
Besides the technical complexity of integrating network models, we have the issue of confidentiality. System operators, the instances responsible for safe operation of their electricity grid, are not willing or not allowed to share network information with other system operators. One can reason that the ongoing energy transition and electrification is going to push the limits of conventional models until they do not suffice anymore. It is probable that legislation and current behaviour will then follow the necessary change towards the use of integrated network models.

The study of integrated network models is an emerging field. A literature review shows that multiple approaches exist that can roughly be categorized into 1) co-simulation frameworks that combine multiple domains that can be studied using different tools and 2) stand-alone analysis frameworks that study integrated network models in one software program [13]. The focus of this work is on the analysis of stand-alone frameworks. Although co-simulation frameworks are ideal for simultaneous analysis of large transmission and distribution networks (100s to 1000s of buses) due to their modular nature and suitability for HPC architectures [2], we expect a competitive advantage for stand-alone models in the near future. Efficiently integrated stand-alone models require significantly less communication and should therefore be compatible with co-simulation techniques. Thus far, several stand-alone integration techniques have been developed and tested on small-size transmission and distribution networks in order to check their feasibility [14] [15]. In this work, we compare the performance of the existing stand-alone methods on

convergence rate and CPU-time and their ability to be efficiently scaled to large-size networks by applying them on several transmission-distribution networks. The contributions of this work can be summarized as follows:

- An extensive description of existing stand-alone methods that have been categorized according their modeling and integration approach;
- A comparison of these methods using the Matpower library [16] in which several test-cases are created to simulate the convergence behavior, where special attention is paid to CPU-time and number of iterations;
- An analysis of convergence characteristics under varying circumstances such as a high level of distributed generation and the integration of multiple distribution networks into one transmission-network;
- An insight into how these methods should adapt according to HPC applications in order to solve realistically sized networks (up to 1000000s buses).

2 Characterization of the power flow problem

The steady-state power flow problem is the problem of determining the voltages V in a network, given the specified power[1] $S = P + \iota Q$ and current I. V and I are related by Ohm's Law, $I = YV$, and S and V are related by $S = VI^*$. Y represents the admittance of a power cable. Power is generated in three phases leading to three sinusoidal functions that describe phase a, b, and c of the voltage and of the current. The voltage and current are both expressed in phasor notation:

$$V_p = |V|_p \exp(\iota\delta_{V_p} - \phi_p), \tag{1}$$
$$I_p = |I|_p \exp(\iota\delta_{I_p} - \phi_p), \quad p \in \{a, b, c\}, \tag{2}$$

where $|\cdot|$ describes the phasor magnitude, δ_* the phase angle, and ϕ_* the phase shift. Phasors are often expressed as $V = \{|V|, \delta\}$. Current is never specified in an electricity system, therefore we substitute Ohm's Law into $S = VI^*$ and get a nonlinear equation for S, the three-phase nonlinear power flow equation, described as follows:

$$S_p = V_p(\mathbf{Y}V)^*_p, \quad p \in \{a, b, c\}. \tag{3}$$

We represent an electricity network as a graph consisting of buses $i = 1, .., N$ and branches (named after the two surrounding buses). These buses are either a load bus (PQ bus), a generator bus (PV bus), or a reference bus, depending on the information we know at that point. The loads in a network are modeled as PQ buses, loads consume power and at this bus, the active (P) and reactive power (Q) are specified. Generators are modeled as PV buses, except for the first generator in a network, this bus is modeled as the slack bus. Generators supply power and at this bus, the active power (P) and voltage magnitude ($|V|$) are specified. At a slack bus, the voltage magnitude and angle are specified. This is summarized in

Table 1: Bustypes in a network and the information we know and not know at each bus i.

bus type	known	unknown
PQ-bus	$P_i,\ Q_i$	$\delta_i,\ \lvert V_i\rvert$
PV-bus	$P_i,\ \lvert V_i\rvert$	$Q_i,\ \delta_i$
slack bus	$\delta_i,\ \lvert V_i\rvert$	$P_i,\ Q_i$

table 1. We scale all the engineering quantities in the power system to per-unit (pu) quantities by dividing them by their base value. In this way, we bring the voltage in a narrow range close to unity to eliminate erroneous values [4].
Equation (3) is a nonlinear equation so we solve it using iterative methods. At each node i, we solve the following equation for the unknown quantities:

$$S_i = V_i \sum_{k=1}^{N} \mathbf{Y}_{ik}^{*} V_k^{*} \tag{4}$$

The nodal admittance matrix $\mathbf{Y}_{ij}$ consists of admittance y_{ij} of a line between node i and j and nodal shunt susceptance b_c. Line admittance consists of a real and imaginary part: $y_{ij} = 1/z_{ij} = 1/(r_{ij} + \iota x_{ij})$, z being impedance, r being resistance and x being reactance. The nodal admittance matrix relating node i and j looks as the following:

$$\mathbf{Y}_{ij} = \begin{bmatrix} (y_{ij} + \iota\frac{b_c}{2})\frac{1}{\tau^2} & -y_{ij}\frac{1}{\tau \exp(-\iota\theta_s)} \\ -y_{ij}\frac{1}{\tau \exp(\iota\theta_s)} & y_{ij} + \iota\frac{b_c}{2} \end{bmatrix} = \begin{bmatrix} Y_{11} & Y_{12} \\ Y_{21} & Y_{22} \end{bmatrix}_{ij}$$

The parameters θ_s and τ are the transformer's phase-shift angle and tap ratio, when there is no transformer between two nodes but just a normal power cable, $\theta_s = 0$ and $\tau = 1$.

3 Electricity networks

An electricity network consists of one transmission and several distribution networks. The design and characteristics of these types are different and therefore require different approaches to solve equation (3).

3.1 Transmission networks: single-phase representation

The transmission network is the high-voltage network, responsible for the transportation of power over large distances. It is a balanced system which means that the three phases $a,\ b$, and c of the generated power are equal in magnitude and equal in phase-shift (ϕ). For a voltage V this means that $|V|_a = |V|_b = |V|_c$ and $\phi_{ab} = \phi_{bc} = \phi_{ca} = \frac{2}{3}\pi$. To simplify and speed-up the computations in the

[1] We use the subscript ι as the imaginary unit.

transmission network, they only calculate V_a and deduct the other two phases from here. This changes (3) into the following:

$$S_p = V_p(YV)_p^*, \quad p \in \{a, b, c\} \quad \Rightarrow \quad S_a = V_a(YV)_a^*. \tag{5}$$

We use Newton-Raphson power mismatch (NR-power) to compute unknown quantities at each bus i. NR-power computes V_i using the following power mismatch formulation:

$$\Delta S_i = S_{s,i} - S(V_i) \approx 0. \tag{6}$$

S_s is the specified power, the known information at generator and load nodes: $S_s = S_g - S_d$, subscript g representing the generator buses and d the load buses. $S(V)$ is the injected power, $S(V) = V(\mathbf{Y}V)^*$. The complex power S is split into an active and reactive part and combined to form the power mismatch vector F,

$$F(V) = \begin{bmatrix} \Delta P \\ \Delta Q \end{bmatrix} = \begin{bmatrix} P_s - P(V) \\ Q_s - Q(V) \end{bmatrix}. \tag{7}$$

We denote the state variables V by x, $x := V = \{|V|, \delta\}$. We compute V in an iterative manner using the Jacobian J of the power mismatch vector:

$$\Delta x^\nu = -\mathbf{J}^{-1}(x^\nu)F(x^\nu), \tag{8}$$

$$x^{\nu+1} = x^\nu + \Delta x^\nu, \tag{9}$$

where the Jacobian is represented as follows:

$$\mathbf{J}(x) = \begin{bmatrix} \frac{\partial P}{\partial \delta} & \frac{\partial P}{\partial |V|} \\ \frac{\partial Q}{\partial \delta} & \frac{\partial Q}{\partial |V|} \end{bmatrix}.$$

We repeat this until the norm of the power mismatch vector $|F|_\infty$ is lower than a certain tolerance value ϵ. We choose $\epsilon = 10^{-5}$ and start with a flat profile as initial guess: $V^0 = 0$. The Newton-Raphson algorithm is as follows:

Algorithm 3.1 The Newton-Raphson iterative method

1: Set $\nu = 0$ and choose appropriate starting value $\mathbf{x}^0$;
2: Compute $F(x^\nu)$;
3: Test convergence: If $|F(x^\nu)|_\infty \leq \epsilon$ then x^ν is the solution, Otherwise continue.
4: Compute the Jacobian matrix $\mathbf{J}(x^\nu)$;
5: Update the solution:

$$\Delta x^\nu = -\mathbf{J}^{-1}(x^\nu)F(x^\nu)$$
$$x^{\nu+1} = x^\nu + \Delta x^\nu$$

6: Update iteration counter $\nu + 1 \rightarrow \nu$, go to step 2.

3.2 Distribution networks: three-phase representation

Distribution systems are unbalanced: the three phases are not equal in magnitude nor in phase-shift. This requires us to compute all the three phases in every iteration when solving equation (3). We use Newton-Raphson Three-Phase Current Injection Method (NR-TCIM) [5] to solve distribution networks. Instead of applying the standard Newton-Raphson method to power mismatches, Ohm's Law is directly used resulting in the current mismatch vector:

$$F(x) = \begin{bmatrix} \Delta I^{Re,abc}(x) \\ \Delta I^{Im,abc}(x) \end{bmatrix} = \begin{bmatrix} I_s^{Re,abc} - I^{Re,abc}(x) \\ I_s^{Im,abc} - I^{Im,abc}(x) \end{bmatrix}. \tag{10}$$

The specified current I_s and computed current $I(V)$ are calculated using the injected complex power and Ohm's Law:

$$I_{s,i} = \left(\frac{\overline{S_s}}{\overline{V}}\right)_i \quad \text{and} \quad I(V)_i = \mathbf{Y}V_i \tag{11}$$

The Jacobian is formed by taking the derivative of the real and imaginary current mismatch with respect to the real and imaginary voltage.

3.3 Modeling elements in three-phase configuration

An electricity network models consists of nodal and series elements. Loads, generators, and shunts are nodal elements and are taken into account in the complex power vector $\mathbf{S}$. Transformers, line elements, and regulators are placed in series. They are accounted for in the Y_{bus} matrix. Regulators are elements that are placed alone the distribution feeder to regulate the voltage profile of the feeder.

3.3.1 Loads and shunts

Loads are modeled as buses where active and reactive power (P and Q) are specified. They are modeled as a function of the voltage in which the load-model type determines the relation between power and voltage. Three types exist: the constant power (P), constant current (I), and constant impedance model (Z). Together called: ZIP-load models.

1. Constant Power models (P): power is independent of the change in voltage magnitude, which is expressed as:

   $$\frac{P}{P_0} = 1 \quad \text{and} \quad \frac{Q}{Q_0} = 1$$

   Constant power loads draw the same power from its source even if the source changes voltage.

2. Constant Current models (I): power is related to the voltage magnitude as:

   $$\frac{P}{P_0} = \frac{|V|}{|V_0|} \quad \text{and} \quad \frac{Q}{Q_0} = \frac{|V|}{|V_0|}$$

A constant current load varies its internal resistance according to the voltage which is being fed to it in order to achieve a constant current despite fluctuations in the source voltage.

3. Constant Impedance models (Z): power is related to the square of the voltage magnitude:
$$\frac{P}{P_0} = (\frac{|V|}{|V_0|})^2 \quad \text{and} \quad \frac{Q}{Q_0} = (\frac{|V|}{|V_0|})^2$$
A constant impedance load presents the same impedance even when voltage is fluctuating.

The entities P_0 and Q_0 are the specified power ratings and $|V_0|$ is the nominal voltage magnitude. In p.u. calculations, $|V_0|$ is often equal to 1.

Loads are physically connected in a grounded Wye or ungrounded Delta configuration. In the grounded Wye configuration all the three phases are connected to a single neutral point. This neutral point is connected to the ground by a fourth wire: the neutral conductor. The voltage is specified line-to-neutral. In an ungrounded Delta configuration the loads are connected phase-to-phase without a neutral conductor. Here, the voltage is specified phase-to-phase, also called line-to-line. The line-to-line voltages of a three-phase Delta-configuration are: V^{ab}, V^{bc}, and V^{ca}. The line-to-line voltages and line-to-neutral voltages (V^a, V^b, and V^c) are related as follows:

$$V^{ab} = V^a - V^b, \tag{12}$$
$$V^{bc} = V^b - V^c, \tag{13}$$
$$V^{ca} = V^c - V^a. \tag{14}$$
$$\tag{15}$$

The line-to-neutral currents are related to line-to-line voltages according:

$$I^a = I^{ab} - I^{ca}, \tag{16}$$
$$I^b = I^{bc} - I^{ab}, \tag{17}$$
$$I^c = I^{ca} - I^{bc}. \tag{18}$$

In the following lines we clarify the relationship of the ZIP-load models in a Wye and Delta configuration.

Wye - P We know that power is independent of voltage magnitude:

$$\frac{P}{P_0} = 1,\ \frac{Q}{Q_0} = 1 \ \Leftrightarrow\ S := P + \iota Q = P_0 + \iota Q_0 \tag{19}$$

For phases a, b, and c this means that for each load bus i the active and reactive power are expressed as follows:

$$\begin{bmatrix} S^a \\ S^b \\ S^c \end{bmatrix}_i := \begin{bmatrix} P^a + \iota Q^a \\ P^b + \iota Q^b \\ P^c + \iota Q^c \end{bmatrix}_i = \begin{bmatrix} (P_0^a + \iota Q_0^a) \\ (P_0^b + \iota Q_0^b) \\ (P_0^c + \iota Q_0^c) \end{bmatrix}_i \tag{20}$$

Wye - I Constant current load models vary their power S with voltage magnitude, leading to the following relationship:

$$\frac{P}{P_0} = |V|,\ \frac{Q}{Q_0} = |V| \ \Leftrightarrow\ S := P + \iota Q = (P_0 + \iota Q_0)|V| \tag{21}$$

For phases a, b, and c this means that for each load bus i the active and reactive power are expressed as follows:

$$\begin{bmatrix} S^a \\ S^b \\ S^c \end{bmatrix}_i := \begin{bmatrix} P^a + \iota Q^a \\ P^b + \iota Q^b \\ P^c + \iota Q^c \end{bmatrix}_i = \begin{bmatrix} (P_0^a + \iota Q_0^a)(\frac{|V^a|}{|V_0^a|}) \\ (P_0^b + \iota Q_0^b)(\frac{|V^b|}{|V_0^b|}) \\ (P_0^c + \iota Q_0^c)(\frac{|V^c|}{|V_0^a|}) \end{bmatrix}_i \tag{22}$$

Wye - Z Constant impedance models vary their power with the square of voltage magnitude, leading to the following:

$$\frac{P}{P_0} = |V|^2,\ \frac{Q}{Q_0} = |V|^2 \ \Leftrightarrow\ S := P + \iota Q = (P_0 + \iota Q_0)|V|^2 \tag{23}$$

For phases a, b, and c this means that for each load bus i the active and reactive power are expressed as follows:

$$\begin{bmatrix} S^a \\ S^b \\ S^c \end{bmatrix}_i := \begin{bmatrix} P^a + \iota Q^a \\ P^b + \iota Q^b \\ P^c + \iota Q^c \end{bmatrix}_i = \begin{bmatrix} (P_0^a + \iota Q_0^a)(\frac{|V^a|}{|V_0^a|})^2 \\ (P_0^b + \iota Q_0^b)(\frac{|V^b|}{|V_0^b|})^2 \\ (P_0^c + \iota Q_0^c)(\frac{|V^c|}{|V_0^a|})^2 \end{bmatrix}_i \tag{24}$$

We solve the three-phase distribution systems with the NR-TCIM method, which implies that we need the specified currents I_s in our mismatch equation (eq: 10) instead of specified powers. As currents are never measured in a power system, they are conducted from the specified power according the relationship:

$$S = VI^* \ \Leftrightarrow\ I = (\frac{S}{V})^* \tag{25}$$

If we divide the expressions of the loads S by V and take the conjugate of this new relation we get the load models expressions in terms of specified current:

Wye - P

$$I := (\frac{S}{V})^* = (\frac{P_0 + \iota Q_0}{V})^* \tag{26}$$

Or in three-phase matrix:

$$\begin{bmatrix} I^a \\ I^b \\ I^c \end{bmatrix}_i = \begin{bmatrix} (\frac{P^a + \iota Q^a}{V^a})^* \\ (\frac{P^b + \iota Q^b}{V^b})^* \\ (\frac{P^c + \iota Q^c}{V^c})^* \end{bmatrix}_i \tag{27}$$

Wye - I

$$I := (\frac{S|V|}{V})^* = (P_0 + \iota Q_0)^* \frac{|V|}{V^*} = (P_0 + \iota Q_0)^* \frac{V}{|V|} \tag{28}$$

Or in three-phase matrix:

$$\begin{bmatrix} I^a \\ I^b \\ I^c \end{bmatrix}_i = \begin{bmatrix} (P^a + \iota Q^a)^* \frac{V^a}{|V^a|} \\ (P^b + \iota Q^b) \frac{V^b}{|V^b|} \\ (P^c + \iota Q^c)^* \frac{V^c}{|V^c|}) \end{bmatrix}_i \tag{29}$$

Wye - Z

$$I := (\frac{S|V|^2}{V})^* = (P_0 + \iota Q_0)^* \frac{|V|^2}{V^*} = (P_0 + \iota Q_0)^* \frac{VV^*}{V^*} = (P_0 + \iota Q_0)^* V \tag{30}$$

Or in three-phase matrix:

$$\begin{bmatrix} I^a \\ I^b \\ I^c \end{bmatrix}_i = \begin{bmatrix} (P^a + \iota Q^a)^* V^a \\ (P^b + \iota Q^b)^* V^b \\ (P^c + \iota Q^c)^* V^c \end{bmatrix}_i \tag{31}$$

Delta loads Delta loads are expressed by line-to-line voltages and currents while we need line-to-neutral currents in our calculations. We express the line-to-neutral currents directly for the three load models using

$$I^a = I^{ab} - I^{ca}, \tag{32}$$

$$I^b = I^{bc} - I^{ab}, \tag{33}$$

$$I^c = I^{ca} - I^{bc}. \tag{34}$$

Delta - P

$$\begin{bmatrix} I^a \\ I^b \\ I^c \end{bmatrix}_i := \begin{bmatrix} I^{ab} - I^{ca} \\ I^{bc} - I^{ab} \\ I^{ca} - I^{bc} \end{bmatrix}_i = \begin{bmatrix} (\frac{P^{ab} + \iota Q^{ab}}{V^a - V^b})^* - (\frac{P^{ca} + \iota Q^{ca}}{V^c - V^a})^* \\ (\frac{P^{bc} + \iota Q^{bc}}{V^b - V^c})^* - (\frac{P^{ab} + \iota Q^{ab}}{V^a - V^b})^* \\ (\frac{P^{ca} + \iota Q^{ca}}{V^c - V^a})^* - (\frac{P^{bc} + \iota Q^{bc}}{V^b - V^c})^* \end{bmatrix}_i \tag{35}$$

Delta - I

$$\begin{bmatrix} I^a \\ I^b \\ I^c \end{bmatrix}_i = \begin{bmatrix} (P^{ab} + \iota Q^{ab})^* \frac{(V^a - V^b)}{|V^a - V^b|} - (P^{ca} + \iota Q^{ca})^* \frac{(V^c - V^a)}{|V^c - V^a|} \\ (P^{bc} + \iota Q^{bc})^* \frac{(V^b - V^c)}{|V^b - V^c|} - (P^{ab} + \iota Q^{ab})^* \frac{(V^a - V^b)}{|V^a - V^b|} \\ (P^{ca} + \iota Q^{ca})^* \frac{(V^c - V^a)}{|V^c - V^a|} - (P^{bc} + \iota Q^{bc})^* \frac{(V^b - V^c)}{|V^b - V^c|} \end{bmatrix}_i \tag{36}$$

Delta - Z

$$\begin{bmatrix} I^a \\ I^b \\ I^c \end{bmatrix}_i = \begin{bmatrix} (P^{ab} + \iota Q^{ab})^* (V^a - V^b) - (P^{ca} + \iota Q^{ca})^* (V^c - V^a) \\ (P^{bc} + \iota Q^{bc})^* (V^b - V^c) - (P^{ab} + \iota Q^{ab})^* (V^a - V^b) \\ (P^{ca} + \iota Q^{ca})^* (V^c - V^a) - (P^{bc} + \iota Q^{bc})^* (V^b - V^c) \end{bmatrix}_i \tag{37}$$

Overview of load models We give an overview line-to-neutral currents I_i^p, $p \in \{a, b, c\}$ for the three static load models (P, I, and Z) in Wye and Delta configuration.

Table 2: Specified line-to-neutral currents I_i^p of load bus i in Wye and Delta configuration, given for different load models (ZIP).

	Y	Δ
load model	Wye	Delta
Z	$\begin{bmatrix} (P^a + \iota Q^a)^* V^a \\ (P^b + \iota Q^b)^* V^b \\ (P^c + \iota Q^c)^* V^c \end{bmatrix}_i$	$\begin{bmatrix} (P^{ab} + \iota Q^{ab})^* (V^a - V^b) - (P^{ca} + \iota Q^{ca})^* (V^c - V^a) \\ (P^{bc} + \iota Q^{bc})^* (V^b - V^c) - (P^{ab} + \iota Q^{ab})^* (V^a - V^b) \\ (P^{ca} + \iota Q^{ca})^* (V^c - V^a) - (P^{bc} + \iota Q^{bc})^* (V^b - V^c) \end{bmatrix}_i$
I	$\begin{bmatrix} (P^a + \iota Q^a)^* \frac{V^a}{\lvert V^a \rvert} \\ (P^b + \iota Q^b) \frac{V^b}{\lvert V^b \rvert} \\ (P^c + \iota Q^c)^* \frac{V^c}{\lvert V^c \rvert}) \end{bmatrix}_i$	$\begin{bmatrix} (P^{ab} + \iota Q^{ab})^* \frac{(V^a - V^b)}{\lvert V^a - V^b \rvert} - (P^{ca} + \iota Q^{ca})^* \frac{(V^c - V^a)}{\lvert V^c - V^a \rvert} \\ (P^{bc} + \iota Q^{bc})^* \frac{(V^b - V^c)}{\lvert V^b - V^c \rvert} - (P^{ab} + \iota Q^{ab})^* \frac{(V^a - V^b)}{\lvert V^a - V^b \rvert} \\ (P^{ca} + \iota Q^{ca})^* \frac{(V^c - V^a)}{\lvert V^c - V^a \rvert} - (P^{bc} + \iota Q^{bc})^* \frac{(V^b - V^c)}{\lvert V^b - V^c \rvert} \end{bmatrix}_i$
P	$\begin{bmatrix} (\frac{P^a + \iota Q^a}{V^a})^* \\ (\frac{P^b + \iota Q^b}{V^b})^* \\ (\frac{P^c + \iota Q^c}{V^c})^* \end{bmatrix}_i$	$\begin{bmatrix} (\frac{P^{ab} + \iota Q^{ab}}{V^a - V^b})^* - (\frac{P^{ca} + \iota Q^{ca}}{V^c - V^a})^* \\ (\frac{P^{bc} + \iota Q^{bc}}{V^b - V^c})^* - (\frac{P^{ab} + \iota Q^{ab}}{V^a - V^b})^* \\ (\frac{P^{ca} + \iota Q^{ca}}{V^c - V^a})^* - (\frac{P^{bc} + \iota Q^{bc}}{V^b - V^c})^* \end{bmatrix}_i$

3.3.2 Transformers

Transformers are placed between two networks that have different voltage levels. The primary side (p) of the transformer is connected to the higher voltage network and the secondary side (s) is connected to the lower voltage level. The transformer in a power system is represented by two blocks:

- An admittance matrix block, Y_T^{abc}, consisting of per-unit leakage admittance y_t, and
- A shunt block that models core losses. The shunt block can be represented by voltage dependent loads and follow the representation in Table 2.

The admittance matrix block is given in a similar manner as the Y_{bus} matrix of a distribution cable, but now consisting of leakage admittance of the transformer:

$$Y_T^{abc} = \begin{bmatrix} Y_{pp}^{abc} & Y_{ps}^{abc} \\ Y_{sp}^{abc} & Y_{ss}^{abc} \end{bmatrix}. \tag{38}$$

Each block Y_{ij}^{abc}, $i, j \in \{p, s\}$ has a different configuration. This configuration depends on the connection of the transformer and is either one of the three following blocks:

$$Y_1 = \begin{bmatrix} y_t & 0 & 0 \\ 0 & y_t & 0 \\ 0 & 0 & y_t \end{bmatrix}, \quad Y_2 = \tfrac{1}{3} \begin{bmatrix} 2y_t & -y_t & -y_t \\ -y_t & 2y_t & -y_t \\ -y_t & -y_t & 2y_t \end{bmatrix}, \quad \text{and} \quad Y_3 = \tfrac{1}{\sqrt{3}} \begin{bmatrix} -y_t & y_t & 0 \\ 0 & -y_t & y_t \\ y_t & 0 & -y_t \end{bmatrix}. \tag{39}$$

Table 3 represents the corresponding block per transformer configuration.
The pu leakage admittance y_t consists of resistance r and reactance x. The equations should be scaled according the correct base quantities in order to match the different pu-systems. The pu leakage admittance results in:

$$y_t = \frac{1}{z_t}, \quad \text{where } z_t = (r + \iota x)(\frac{V_{low}}{V_{base}})^2 \frac{S_{base}}{S_t}, \tag{40}$$

where r and x are given in fractions. V_{low} is the voltage at the secondary level of the transformer, and S_T is apparent power of the transformer, expressed in volt-ampere. V_{base} is always given in line-to-line and should be converted to line-to-neutral by dividing it by $\sqrt{3}$, in order to match the calculations.

Table 3: Specified line-to-neutral currents of load bus i in Wye and Delta configuration, given for different load models (ZIP).

Transformer model					
Primary	Secondary	Y_{pp}^{abc}	Y_{ps}^{abc}	Y_{sp}^{abc}	Y_{ss}^{abc}
Wye-G	Wye-G	Y_1	$-Y_1$	$-Y_1$	Y_1
Wye-G	Wye	Y_2	$-Y_2$	$-Y_2$	Y_2
Wye-G	Delta	Y_1	Y_3	Y_3^T	Y_2
Wye	Wye-G	Y_2	$-Y_2$	$-Y_2$	Y_2
Wye	Wye	Y_2	$-Y_2$	$-Y_2$	Y_2
Wye	Delta	Y_2	Y_3	Y_3^T	Y_2
Delta	Wye-G	Y_2	Y_3^T	Y_3	Y_1
Delta	Wye	Y_2	Y_3^T	Y_3	Y_2
Delta	Delta	Y_2	$-Y_2$	$-Y_2$	Y_2

3.3.3 Step-Voltage Regulators

Step-Voltage Regulators (SVRs) are installed along distribution feeders, often after the substation, but also at other locations, to control the voltage along the feeder and to keep it within an acceptable range. As the voltages along a distribution feeder can vary, it is important to keep it within an acceptable range. An SVR consists of a sequence of autotransformers and load tap changing mechanisms [17]. The taps of the transformers are responsible for the voltage level at the secondary side, the output voltage. This voltage is measured: If it falls outside the safety region, the tap ratios are changed automatically to adjust this voltage level. Standard SVRs allow a total of $\pm 10\%$ voltage change, usually achieved in 32 steps. This means that each tap changes the voltage with 0.000625 per unit in an up or down direction [17]. In our load-flow computations, we are not implementing an SVR that changes its tap ratio automatically. We pre-determine the safe tap-ratios based on output data of openDSS. With these data we model the SVR directly.
An SVR is modeled as a series block that is placed between any connected pair of buses (n,m). The voltages and currents of the primary (bus n) and secondary

side (bus m) of the SVR are related via matrices: A_V, A_I, and $Z_R \in \mathbb{C}^{6x6}$. The first one represents voltage gain, the second current gain, and the last impedance. A_I and A_V consists of effective regulator ratio a_R and Z_R consists of pu series impedance z_R of the SVR [18]. The regulator ratio, a_R, is expressed as a function of the tap ratio:

$$a_R = 1 \pm 0.000625tap, \tag{41}$$

where *tap* is the tap-ratio of the SVR. The minus sign in this equation applies for the raise position and the positive sign for the lower position.
Three-phase SVRs are commonly configured as Wye, closed-delta, and open-delta connections. Just like transformers, these configurations determine the entities of the three blocks A_I, A_V, and Z_R. Furthermore, it holds that:

$$A_V^- - 1 = A_I^T. \tag{42}$$

These three blocks form the SVR-admittance matrix, Y_R^{abc}. The admittance matrix Y_R^{abc} looks as follows:

$$Y_R^{abc} = \begin{bmatrix} A_I F_R^{-1} Y_{nn}^{abc} A_I^T & -A_I F_R^{-1} Y_{nm}^{abc} \\ -Y_{mn}^{abc} F_R^{-T} A_I^T & Y_{mm}^{abc} - Y_{mn}^{abc} A_I^T Z_R A_I F_R^{-1} Y_{nm}^{abc} \end{bmatrix} \tag{43}$$

Y_{ij}^{abc}, $i,j \in \{n,m\}$ is the admittance of the distribution line along which the regulator is placed. F_R and F_R^{-T} are defined as follows:

$$F_R = \mathbf{I}_{3\times 3} + Y_{nn}^{abc} A_I^T Z_R A_I, \tag{44}$$

$$F_R^{-T} = \mathbf{I}_{3\times 3} - A_I^T Z_R A_I F_R^{-1} Y_{nn}^{abc}. \tag{45}$$

We list the entities of the blocks A_I, A_V, and Z_R, that depend on the SVR configuration, in Table 4. More information on how to derive these entities can be found in [18].

Table 4: Specified line-to-neutral currents of load bus i in Wye and Delta configuration, given for different load models (ZIP).

SVR connection	A_I	A_V	Z_R
Wye	$\begin{bmatrix} \frac{1}{a_{R_a}} & 0 & 0 \\ 0 & \frac{1}{a_{R_b}} & 0 \\ 0 & 0 & \frac{1}{a_{R_c}} \end{bmatrix}$	$\begin{bmatrix} a_{R_a} & 0 & 0 \\ 0 & a_{R_b} & 0 \\ 0 & 0 & a_{R_c} \end{bmatrix}$	$\begin{bmatrix} Z_{R_a} & 0 & 0 \\ 0 & Z_{R_b} & 0 \\ 0 & 0 & Z_{R_c} \end{bmatrix}$
Closed-Delta	$\begin{bmatrix} a_{R_{ab}} & 0 & 1-a_{R_{ca}} \\ 1-a_{R_{ab}} & a_{R_{bc}} & 0 \\ 0 & 1-a_{R_{bc}} & a_{R_{ca}} \end{bmatrix}^{-1}$	$\begin{bmatrix} a_{R_{ab}} & 1-a_{R_{ab}} & 0 \\ 0 & a_{R_{bc}} & 1-a_{R_{bc}} \\ 1-a_{R_{ca}} & 0 & a_{R_{ca}} \end{bmatrix}$	$\begin{bmatrix} Z_{R_{ab}} & 0 & 0 \\ 0 & Z_{R_{bc}} & 0 \\ 0 & 0 & Z_{R_{ca}} \end{bmatrix}$
Open-Delta	$\begin{bmatrix} \frac{1}{a_{R_{ab}}} & 0 & 0 \\ 1-\frac{1}{a_{R_{ab}}} & 1 & 1-\frac{1}{a_{R_{cb}}} \\ 0 & 0 & \frac{1}{a_{R_{cb}}} \end{bmatrix}$	$\begin{bmatrix} a_{R_{ab}} & 1-a_{R_{ab}} & 0 \\ 0 & 1 & 0 \\ 0 & 1-a_{R_{cb}} & a_{R_{cb}} \end{bmatrix}$	$\begin{bmatrix} Z_{R_{ab}} & 0 & 0 \\ 0 & 0 & 0 \\ 0 & 0 & Z_{R_{cb}} \end{bmatrix}$

Ideal SVRs If the auto-transformer of the SVR is ideal, the tap-ratio is equal to 0 and the impedance matrix Z_R is equal 0. This results into F_R being the identity matrix: $\mathbf{I}_{3\times3}$. The admittance matrix of an ideal SVR becomes the following:

$$Y^{abc}_{R,ideal} = \begin{bmatrix} A_I Y^{abc}_{nn} A_I^T & -A_I Y^{abc}_{nm} \\ -Y^{abc}_{mn} A_I^T & Y^{abc}_{mm} \end{bmatrix}. \tag{46}$$

4 Integrating transmission and distribution networks

We have a single-phase transmission system described by the following power flow relation:

$$S^a_i = V^a_i \overline{I^a_i} = V^a_i \sum_{k=1}^{N} \overline{Y^a_{ik} V^a_k}, \tag{47}$$

and a three-phase distribution system, described by the following power flow relation:

$$S^p_i = V^p_i \overline{I^p_i} = V^p_i \sum_{k=1}^{N} \sum_{q=a,b,c} \overline{Y^{pq}_{ik} V^q_k}, \quad p \in \{a,b,c\}. \tag{48}$$

These two networks are connected to each other via a substation. A dimension mismatch takes place at this substation, depicted in figure 1. Table 5 shows the single-phase and three-phase representation of S, V and Y in the network models. We need integration methods to resolve this mismatch at the substation and solve the power flow problem on the integrated network. The literature suggests two approaches to run stand-alone computations on integrated networks: a unified and a splitting approach, and it suggests two ways of modeling integrated networks: as a homogeneous or as a hybrid network. The unified method solves the integrated system as a whole [14]. The splitting approach appoints the transmission network as the manager[2] and the distribution network as the fellow [19]. It iterates between the two networks and at each iteration, it solves the networks separately. This method

[2]Note that the existing literature talks about master and slaves instead of manager and fellows, but we modernised the naming convention.

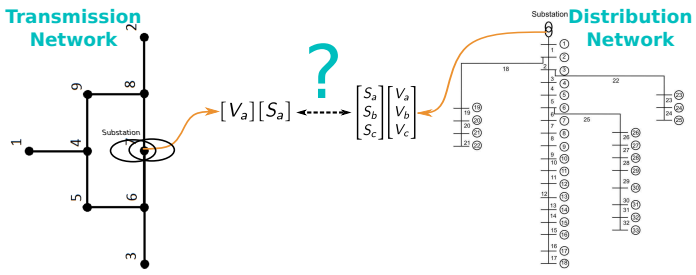

Figure 1: Information mismatch at the substation between a transmission and distribution network

Table 5: Representation of parameters in transmission and distribution network models

parameter	Transmission	Distribution
S_i	$[S_a]_i$	$[S_a \ S_b \ S_c]_i^T$
V_i	$[V_a]_i$	$[V_a \ V_b \ V_c]_i^T$
Y_{ij}	$\begin{bmatrix} Y^a_{11} & Y^a_{12} \\ {\scriptstyle 1\times1} & {\scriptstyle 1\times1} \\ Y^a_{21} & Y^a_{22} \\ {\scriptstyle 1\times1} & {\scriptstyle 1\times1} \end{bmatrix}_{ij}$	$\begin{bmatrix} Y^{abc}_{11} & Y^{abc}_{12} \\ {\scriptstyle 3\times3} & {\scriptstyle 3\times3} \\ Y^{abc}_{21} & Y^{abc}_{22} \\ {\scriptstyle 3\times3} & {\scriptstyle 3\times3} \end{bmatrix}_{ij}$

is similar to the co-simulation approach where the separate domains are solved on its own and coupled using an iterative scheme. We call the unified approach applied to homogeneous networks the full three-phase (F3P) method and applied to hybrid networks the interconnected (IC) method. We call all splitting methods manager-fellow splitting (MFS) methods. We define the MFS-methods based on the network model they are applied to, eg: the splitting approach applied to hybrid networks is called the MFS-hybrid method. Figure 2 gives an overview of the methods.

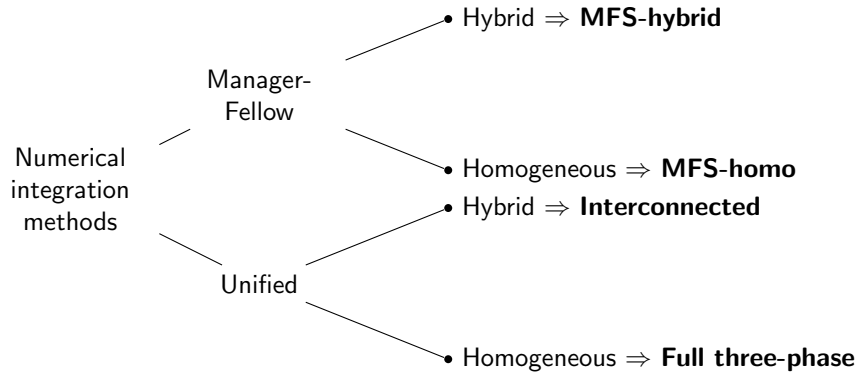

Figure 2: Classification of numerical methods to solve integrated systems.

4.1 Unified methods

Unified methods solve the integrated system using one iterative scheme applied to the entire integrated network. The substation is modeled as a transformer that connects the two networks. The original slack bus of the distribution network becomes a load bus that is connected to the right-hand side of the substation. Any load bus of the transmission network can be connected to the left-hand side of the substation. We solve the entire system using one algorithm.

4.1.1 The full three-phase method

The full three-phase method is the unified method applied on homogeneous networks and a homogeneous network consists of two three-phase networks. Unbalanced distribution networks are by default modeled in three-phase, the transmission networks requires a transformation. This transformation is based on the assumption that the transmission system is balanced: we deduct the phases b and c from the first phase a and we transform the voltage V_a, the complex power S_a, and the admittance Y_a of all the buses $i = 1, ..., N$ to their three-phase equivalents. We transform all the buses $i = 1, .., N$ in the transmission system using transformer matrices:

$$\mathbf{T_1} = \begin{bmatrix} 1 & a^2 & a \end{bmatrix}^T \quad \text{and} \quad \mathbf{T_2} = \begin{bmatrix} 1 & 1 & 1 \end{bmatrix}^T, \quad a = e^{\frac{2}{3}\pi\iota},$$

and identity matrix $\mathbf{I}_{3\times3}$. This results into the following:

$$\mathbf{T_1} \left[V_a\right]_i = \begin{bmatrix} V_a & V_b & V_c \end{bmatrix}_i^T, \tag{49}$$

$$\mathbf{T_2} \left[S_a\right]_i = \begin{bmatrix} S_a & S_b & S_c \end{bmatrix}_i^T, \tag{50}$$

$$\begin{bmatrix} Y_{11}^a \otimes \mathbf{I}_{3\times3} & Y_{12}^a \otimes \mathbf{I}_{3\times3} \\ Y_{21}^a \otimes \mathbf{I}_{3\times3} & Y_{22}^a \otimes \mathbf{I}_{3\times3} \end{bmatrix}_{ij} = \begin{matrix} 3 \\ 3 \end{matrix} \begin{bmatrix} \overset{3}{\mathbf{Y}_{11}^{abc}} & \overset{3}{\mathbf{Y}_{12}^{abc}} \\ \mathbf{Y}_{21}^{abc} & \mathbf{Y}_{22}^{abc} \end{bmatrix}_{ij}. \tag{51}$$

4.1.2 The interconnected method

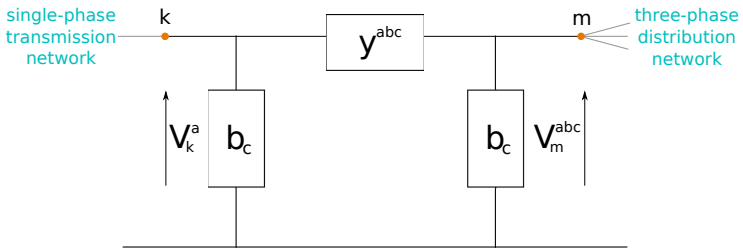

Figure 3: The substation transformer in a hybrid network connecting single-phase bus k and three-phase bus m.

The interconnected method is the unified method applied to hybrid networks. A hybrid network consists of a single-phase transmission part and a three-phase distribution part. The substation transformer, between load bus k of the transmission network and the original slack bus m of the distribution network, connects the information between the two networks. It couples the single-phase quantities at the transmission side to the three-phase quantities at distribution side by transforming the nodal admittance matrix $\mathbf{Y}_{km}$. This is depicted in figure 3. We use three transformer matrices

$$\mathbf{T_1}, \quad \mathbf{T_3} = \frac{1}{3}[1\ a\ a^2], \quad \mathbf{T_4} = \frac{1}{3}\left[1\ 1\ 1\right], \quad \text{and} \quad \mathbf{T_5} = \frac{1}{3}\left[1\ a^2\ a\right], \quad a = e^{\frac{2}{3}\pi\iota},$$

to establish the connection of bus k and m via the admittance matrix $\mathbf{Y}_{km}$. This transformation is based on the assumption that the connecting bus k is perfectly balanced. This means that the single-phase and three-phase quantities are related as the following:

$$\begin{bmatrix} V_a & V_b & V_c \end{bmatrix}_k^T = \mathbf{T_1} \begin{bmatrix} V_a \end{bmatrix}_k, \tag{52}$$

$$\begin{bmatrix} I_a \end{bmatrix}_k = \mathbf{T_3} \begin{bmatrix} I_a & I_b & I_c \end{bmatrix}_k^T, \tag{53}$$

$$\begin{bmatrix} S_a \end{bmatrix}_k = \mathbf{T_4} \begin{bmatrix} S_a & S_b & S_c \end{bmatrix}_k^T. \tag{54}$$

The change of the transformer substation depends on whether the unified system is solved using NR-Power or NR-TCIM. The relations (52), (53), and (54) are substituted in the corresponding power flow equations.

Using current injections The NR-TCIM method uses Ohm's law directly. The relation between node k and m is expressed as follows:

$$I = \mathbf{Y}V \quad \Leftrightarrow \quad \begin{bmatrix} I_k \\ I_m \end{bmatrix} = \begin{bmatrix} Y_{11} & Y_{12} \\ Y_{21} & Y_{22} \end{bmatrix} \begin{bmatrix} V_k \\ V_m \end{bmatrix} \tag{55}$$

If node k and m we're both modeled in three-phase, we know the following:

$$I_k^{abc} = \mathbf{Y}_{11}^{abc} V_k^{abc} + \mathbf{Y}_{12}^{abc} V_m^{abc}, \tag{56}$$

$$I_m^{abc} = \mathbf{Y}_{21}^{abc} V_k^{abc} + \mathbf{Y}_{22}^{abc} V_m^{abc}. \tag{57}$$

We now multiply equation (56) by $\mathbf{T_3}$ to obtain I_k^a:

$$I_k^a = \mathbf{T_3} \mathbf{I}_k^{abc} = \mathbf{T_3} \mathbf{Y}_{11}^{abc} V_k^{abc} + \mathbf{T_3} \mathbf{Y}_{12}^{abc} \mathbf{V}_m^{abc}. \tag{58}$$

We then substitute $\mathbf{V}_k^{abc}$ in equations (58) and (57) by $\mathbf{T_1} V_k^a$ (equation 52):

$$I_k^a = \mathbf{T_3} \mathbf{I}_k^{abc} = \mathbf{T_3} \mathbf{Y}_{11}^{abc} \mathbf{T_1} V_k^a + \mathbf{T_3} \mathbf{Y}_{12}^{abc} \mathbf{V}_m^{abc}, \tag{59}$$

$$\mathbf{I}_m^{abc} = \mathbf{Y}_{21}^{abc} \mathbf{T_1} V_k^a + \mathbf{Y}_{22}^{abc} V_m^{abc}. \tag{60}$$

From (59) and (60) we see that our new nodal admittance matrix becomes:

$$\mathbf{Y}_{km} = \begin{matrix} \\ 1 \\ 3 \end{matrix} \begin{matrix} \begin{matrix} 1 & \quad & 3 \end{matrix} \\ \begin{bmatrix} \mathbf{T_3}[\mathbf{Y}_{11}^{abc}]\mathbf{T_1} & \mathbf{T_3}[\mathbf{Y}_{12}^{abc}] \\ [\mathbf{Y}_{21}^{abc}]\mathbf{T_1} & \mathbf{Y}_{22}^{abc} \end{bmatrix}_{km} \end{matrix} \tag{61}$$

Using power injections We can also start from the power equations. The relation between node k and m is expressed as follows:

$$S = VI^* \quad \Leftrightarrow \quad \begin{bmatrix} S_k \\ S_m \end{bmatrix} = \begin{bmatrix} V_k \\ V_m \end{bmatrix} \begin{bmatrix} I_k \\ I_m \end{bmatrix}^* \tag{62}$$

In the same manner as current injections, we can write this relation in three-phase:

$$S_k^{abc} = V_k^{abc} I_k^{abc*} + V_k^{abc} I_m^{abc*}, \tag{63}$$
$$S_m^{abc} = V_m^{abc} I_k^{abc*} + V_m^{abc} I_m^{abc*}. \tag{64}$$
$$\Leftrightarrow \tag{65}$$
$$S_k^{abc} = \mathsf{diag}(V_k^{abc}) \cdot (\mathbf{Y}_{kk}^{abc} V_k^{abc})^* + \mathsf{diag}(V_k^{abc}) \cdot (\mathbf{Y}_{km}^{abc} V_k^{abc})^*, \tag{66}$$
$$S_m^{abc} = \mathsf{diag}(V_m^{abc}) \cdot (\mathbf{Y}_{mk}^{abc} V_k^{abc})^* + \mathsf{diag}(V_m^{abc}) \cdot (\mathbf{Y}_{mm}^{abc} V_m^{abc})^*. \tag{67}$$

We multiply the first line from the left by $\mathbf{T_4}$ to obtain S_k^a:

$$S_k^a = \mathbf{T_4} S_k^{abc} = \mathbf{T_4}\mathsf{diag}(V_k^{abc}) \cdot (\mathbf{Y}_{kk}^{abc} V_k^{abc})^* + \mathbf{T_4}\mathsf{diag}(V_k^{abc}) \cdot (\mathbf{Y}_{km}^{abc} V_m^{abc})^*. \tag{68}$$

Then, we substitute $V_k^{abc} = \mathbf{T_1} V_k^a$ (equation (52)) in equations (67) and (68) and obtain the following:

$$S_k^a = \mathbf{T_4}\mathsf{diag}(\mathbf{T_1} V_k^a) \cdot (\mathbf{Y}_{kk}^{abc} \mathbf{T_1} V_k^a)^* + \mathbf{T_4}\mathsf{diag}(\mathbf{T_1} V_k^a) \cdot (\mathbf{Y}_{km}^{abc} V_m^{abc})^*, \tag{69}$$
$$S_m^{abc} = \mathsf{diag}(V_m^{abc}) \cdot (\mathbf{Y}_{mk}^{abc} \mathbf{T_1} V_k^a)^* + \mathsf{diag}(V_m^{abc}) \cdot (\mathbf{Y}_{mm}^{abc} V_m^{abc})^*. \tag{70}$$

We can rewrite $\mathbf{T_4}\mathsf{diag}(\mathbf{T_1} V_k^a)$, the first part of the rhs in (69), as:

$$\mathbf{T_4}\mathsf{diag}(\mathbf{T_1} V_k^a) \Leftrightarrow \mathbf{T_4}\mathsf{diag}(\mathbf{T_1})\mathsf{diag}(V_k^a) \tag{71}$$
$$= \frac{1}{3}\begin{bmatrix}1 & 1 & 1\end{bmatrix}\begin{bmatrix}1 & 0 & 0\\ 0 & a^2 & 0\\ 0 & 0 & a\end{bmatrix}\mathsf{diag}(V_k^a) \tag{72}$$
$$\Leftrightarrow \underbrace{\frac{1}{3}\begin{bmatrix}1 & a^2 & a\end{bmatrix}}_{\mathbf{T_5}}\mathsf{diag}(V_k^a) \tag{73}$$
$$\Leftrightarrow \mathsf{diag}(V_k^a)\mathbf{T_5}. \tag{74}$$

This results in the following relations for single-phase and three-phase power:

$$S_k^a = \mathsf{diag}(V_k^a) \cdot (\mathbf{T_5}\mathbf{Y}_{kk}^{abc}\mathbf{T_1} V_k^a)^* + \mathsf{diag}(V_k^a) \cdot (\mathbf{T_5}\mathbf{Y}_{km}^{abc} V_m^{abc})^*, \tag{75}$$
$$S_m^{abc} = \mathsf{diag}(V_m^{abc}) \cdot (\mathbf{Y}_{mk}^{abc}\mathbf{T_1} V_k^a)^* + \mathsf{diag}(V_m^{abc}) \cdot (\mathbf{Y}_{mm}^{abc} V_m^{abc})^*. \tag{76}$$

Equations (75), (76) yield the following transformed admittance matrix $\mathbf{Y}_{km}$:

$$\mathbf{Y}_{km} = \begin{matrix}1\\3\end{matrix}\begin{bmatrix}\overset{1}{\mathbf{T_5}[\mathbf{Y}_{kk}^{abc}]\mathbf{T_1}} & \overset{3}{\mathbf{T_5}[\mathbf{Y}_{km}^{abc}]}\\ [\mathbf{Y}_{mk}^{abc}]\mathbf{T_1} & \mathbf{Y}_{mm}^{abc}\end{bmatrix}_{km} \tag{77}$$

4.2 Manager-Fellow splitting methods

In contrast to the unified methods, the MFS-methods keep two separate domains, the transmission and distribution network (or the manager and the fellow), and

introduces an extra iterative scheme between the domains. The two domains have one overlapping bus, this bus is called the boundary bus [19]. The boundary bus is the original slack bus of the distribution system and, like the unified methods, can be any load bus of the transmission system. As the two domains are solved separately, the boundary bus remains the slack bus for the distribution system and the load bus for the transmission system. During one MFS-iteration, we solve the fellow, inject the solution of the boundary bus into the manager, and then solve this system. This iterative process continues until the difference between the boundary bus of the two systems is smaller than a certain tolerance value ϵ. As the boundary bus is the slack bus of the distribution system, it requires the voltage V_B as known information. In the first iteration, we initialize the voltage as $V_B = 1.0$ pu. In the following iterations, we determine the voltage by solving the transmission system. The boundary bus is a load bus for the transmission system and thus requires the complex power as known. We use the output from the distribution system S_B as input for the transmission system. Algorithm 4.1 shows how the iterative scheme of the MFS-method works. As the MFS-method solves the transmission and distribu-

Algorithm 4.1 General algorithmic approach of the manager-fellow splitting method

1: Set iteration counter $\nu = 0$. Initialize the voltage V_B^0 of the fellow.
2: Solve the distribution system. Output: $S_B^{\nu+1}$.
3: Inject $S_B^{\nu+1}$ into the manager.
4: Solve the manager. Output: $V_B^{\nu+1}$.
5: Is $|V_B^{\nu+1} - V_B^{\nu}|_1 > \epsilon$? Repeat step 2 till 5.

tion systems separately, it allows for using different algorithms per domain. In this way, we choose to solve the distribution system with the advantageous NR-TCIM method and the transmission system with the NR-power method.

The MFS-method can be applied to homogeneous networks and to hybrid networks. The first one requiring a transformation of the entire manager domain, the latter requiring a transformation of the boundary bus only.

4.2.1 The MFS-homogeneous method

The MFS-method applied to homogeneous networks requires a transformation of the single-phase transmission system. The balanced transmission system is transformed in the same was as in the F3P-method. The voltage, power, and admittance of all the buses $i = 1, .., N$ are transformed to three-phase equivalents. This idea is summarized in equations (49) - (51) of section 4.1.1.

4.2.2 The MFS-hybrid method

The MFS-method applied to hybrid systems keeps the transmission system in single-phase. Only a transformation of the boundary bus is then required.
As we first solve the distribution system, we receive the complex power S_B as three-phase output, which we have to transform to a single-phase quantity. Once

we have solved the transmission system, we have to transform the single-phase output of the voltage V_B of this system. Here again, we assume that the boundary bus B is balanced. Balanced three-phase power in pu is related to single-phase power in (54) according the following relation:

$$[S_a] = \mathbf{T_4} \begin{bmatrix} S_a & S_b & S_c \end{bmatrix}^T, \quad \mathbf{T_4} = \frac{1}{3} [1\ 1\ 1], \quad \text{and} \quad a = e^{\frac{2}{3}\pi\iota}. \tag{78}$$

The voltage of the boundary bus has the same relation as in (52):

$$\begin{bmatrix} V_a & V_b & V_c \end{bmatrix}_B^T = \mathbf{T_1} \begin{bmatrix} V_a \end{bmatrix}_B, \quad \mathbf{T_1} = [1\ a^2\ a]^T, \quad \text{and} \quad a = e^{\frac{2}{3}\pi\iota}. \tag{79}$$

The MFS-methods do not require a transformation of the nodal admittance matrix. We transform the necessary boundary parameters directly. At every MFS-iteration, we make transformation (78) and (79) after step 2 and step 4 of algorithm 4.1, respectively.

4.2.3 The manager-fellow iterative schemes

In the early work of the research group of [20] are two iterative schemes of the manager-fellow splitting proposed. The first is the Convergence Alternating Iterative (CAI) scheme and the second is the Multistep Alternating Iterative (MAI) scheme. The MAI-scheme is probably disregarded later on as it is not mentioned in more recent work [15] [19] [21]. We explain both schemes, but decided to only include the results of the CAI-scheme in our comparison[3]. In the CAI-scheme, an explicit convergence condition is defined for the fellow and for the manager. The fellow is solved with NR-TCIM, for which we define a tolerance value ϵ_D. Once this system has converged, its boundary output is injected into the manager. The manager is solved using NR-power, for which a (not necessarily) different tolerance value ϵ_T is defined. Once the manager has converged, its boundary output is injected into the fellow. The integrated network is converged once the convergence condition of the MFS-algorithm is met. In the MAI-scheme, first, a maximum number of iterations per separate system is defined, ie: $I_{max,D}$ and $I_{max,T}$. Then, the output of one system is injected into the other as soon this maximum number of iterations has been reached. The convergence of the integrated network is based on the convergence condition of the MFS-algorithm.

Speeding up the CAI-scheme We can speed-up the CAI-scheme if we, at every MFS iteration, initialize the voltages as the output of the previous MFS iteration. In the current suggested schemes, we initialize all the buses, except the boundary bus B, to $V = 1.0$ pu. We can reduce the number of required iterations for the separate systems if we initialize the voltages to its last obtained solution in the previous MFS-iteration, ie: $V_{0,D}^{\nu+1} = V_{I,D}^{\nu}$ and $V_{0,T}^{\nu+1} = V_{I,T}^{\nu}$.

[3]We did implement the MAI-scheme, but these tests showed us that MAI was not beneficial compared to the CAI-scheme and only lead to extra work.

4.3 General expectations of the methods

Based on the theoretical study of the unified and splitting methods and hybrid and homogeneous networks, we have some first expectations about their performances. Firstly, we expect the methods applied on hybrid networks to perform better in terms of CPU-time. Homogeneous network contain a three-phase representation of the transmission network and thus needs to process a larger Jacobian matrix: If we consider a transmission system with N buses, then the Jacobian matrix of a three-phase network will be of size $6N$ x $6N$ compared to a single-phase Jacobian matrix of size $2N$ x $2N$. Secondly, it is possible that we observe a higher number of iterations for the methods applied on hybrid networks. This expectation is based on the assumption that the connection bus at transmission side is completely balanced while it might be unbalanced due to the connection to the unbalanced distribution system.
If we compare the unified and splitting methods, we expect to see an advantage in speed for the unified methods as they only need to solve one system. The splitting methods are advantageous when system operators are not allowed to share complete network information: In the splitting methods, they only need to share information of the connecting boundary bus.

5 Numerical assessment

We implement all previous mentioned methods into the Matpower[4] library. Matpower contains several transmission network test cases. The resources page of IEEE Power & Energy Society contains several distribution network test cases [22]. We create integrated test cases from the existing transmission and distribution test cases. We use the 9-bus, 33-bus, 118-bus, and 3120-bus networks from Matpower as balanced network test cases. All these test-cases, besides the 33-bus network, are transmission networks. The 33-bus is a balanced distribution network. We use the IEEE 13-bus, 37-bus, 123-bus, and 8500-bus data from IEEE P&ES as unbalanced distribution test cases. We change the loading of the 37-bus network by shifting 20% of the original load of phase b equally to phase a and c, like the original authors [14] to create an unbalanced network. We connect the loads of the IEEE test-networks according their given configuration. The loads in the balanced test-networks are originally single-phase loads. In the homogeneous networks, we model them as Wye-P loads. we model the transformers in these networks in a Wye-Wye configuration. We solve the unified methods using NR-TCIM with $\varepsilon = 10^{-5}$ as convergence tolerance value. In the splitting methods, we solve the distribution system using NR-TCIM and a tolerance value of $\varepsilon_D = 10^{-5}$ and the transmission system using NR-P and a tolerance value of $\varepsilon_T = 10^{-5}$. We define the tolerance value of the MFS-method also as $\varepsilon_{MFS} = 10^{-5}$.

We create the following integrated test cases by integrating one balanced network to one or multiple unbalanced networks:

- Test case 1: T9-D13
- Test case 2: D33-D37
- Test case 3: T118-D123
- Test case 4: T3120-D8500
- Test case 5: T9-3D13
- Test case 6: T118-3D123

Connection bus We select a random load bus in the transmission network as the connection bus in the integrated network. We choose bus 7 in the 9-bus network, bus 30 in the 33-bus network, bus 108 in the 118-bus network, and we choose bus 2700 in the 3120-bus network. The original reference bus of the distribution network becomes the connection bus at the distribution side of the integrated network. In the unified methods, this former reference bus must be changed to a load bus. In the splitting method, the distribution reference bus remains a reference bus, initialized by the output it receives from the transmission network. Test cases 5 and 6 have multiple distribution networks connected, eg. test-case 6 consists of one 118-bus transmission network and three 123-bus distribution networks. These networks are connected to the mentioned connection bus and its sequential buses.

[4]MATPOWER is a package of free, open-source Matlab-language M-files for solving steady-state power system simulation and optimization problems [16].

5.1 Results

In this section we compare the integration methods on their numerical performance, which are CPU-time and number of iterations. We share the results in Table 6. We need insight into their numerical performance in order to get an idea which method to choose to solve realistic power flow problems, which are very large electricity networks.

Table 6: Comparison on number of iterations (in case of the MFS-method (I_{MFS}) and the necessary iterations per subdomain (I_T and I_D)), and CPU-time of the integration methods, applied on six test-cases. The top one are methods applied on homogeneous networks. The bottom one is applied on hybrid networks. The slowest CPU-times are printed in boldface.

	F3P		*MFS-homo-CAI*			
	its	*CPU*	I_{MFS}	I_T	I_D	*CPU*
test case	#	*sec*	#	#	#	*sec*
T9-D13 (7)	3	0.016	3	4	4	0.901
D33-D37 (30)	3	0.016	10	3	4	2.641
T118-D123 (108)	4	0.025	3	7	5	0.807
T3120-D8500 (2700)	4	0.367	3	6	5	2.569
T9-3D13 (7-9)	3	0.020	3	4	5	1.49
T118-3D123 (108-110)	4	0.060	3	7	4	1.69
	IC		*MFS-hybrid-CAI*			
	its	*CPU*	I_{MFS}	I_T	I_D	*CPU*
test case	#	*sec*	#	#	#	*sec*
T9-D13 (7)	3	0.015	3	4	4	**1.071**
D33-D37 (30)	3	0.020	11	3	4	**3.818**
T118-D123 (108)	4	0.039	3	4	5	**1.173**
T3120-D8500 (2700)	4	0.612	3	6	5	**3.697**
T9-3D13 (7-9)	3	0.017	3	4	5	**1.79**
T118-3D123 (108-110)	4	0.073	3	4	4	**1.97**

These results show that the difference in CPU-time is most significant between unified and MFS-methods. The MFS-CAI scheme, on average, requires three runs. Per MFS-iteration, two separate systems are solved. If we combine this, we expect to see a difference in CPU-time of around six times, in the advantage of the unified methods. When we compare the results between network models, ie between

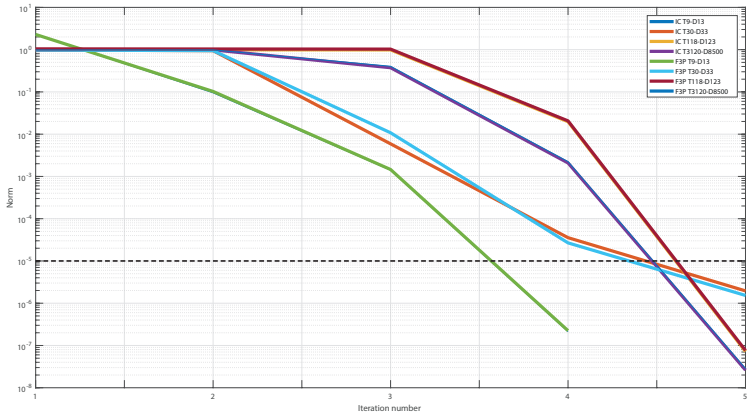

Figure 4: Representation of the norms of $|F|_\infty$ for the interconnected and full three-phase methods for four different test-cases per iteration. The The black dotted line is the tolerance value, ie $\epsilon = 1e-5$.

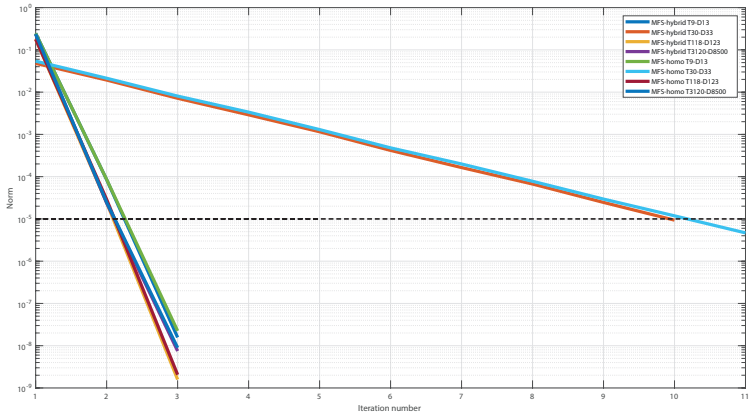

Figure 5: Representation of the relative norms of $|V_B^{\nu+1} - V_B^{\nu}|_\infty$ for the interconnected and full three-phase methods for four different test-cases per iteration. The The black dotted line is the tolerance value, ie $\epsilon = 1e-5$.

hybrid and homogeneous networks, the difference is less significant. For the small test cases, the unified methods are comparable in speed and the MFS methods are comparable in speed. The big test case, T3120-D8500, gives the most significant results. For this test case, the hybrid network methods are 1.5 times faster than the homogeneous methods. Over-all, the MFS-homo-CAI methods perform the least and the IC methods perform the best, in line with our expectations.

If we compare the number of iterations, we see that there is hardly any difference among unified methods and among MFS-methods. Note also that adding multiple distribution networks to a transmission network, does not influence the total number of iterations.

6 Conclusion

We have reviewed and assessed two types of integration methods to solve the power flow problem. We classified them as unified and splitting methods and applied them on hybrid and homogeneous networks. This resulted in four different methods as starting point of our numerical comparison study. We analyzed the numerical performance, ie CPU-time and number of iterations to reach convergence.
From this assessment we can conclude that the unified methods are most favorable in sense of CPU-time compared to splitting methods, in line with the expectations we stated in section 4.3. The differences within the unified methods are less significant than we expected. We argued that the increase in size of the Jacobian would have resulted in increase of CPU-time. Only in the bigger test-case T3120-D8500 that the difference becomes significant: The F3P-method is around 1.5 times as slow as the Interconnected method.
Based on these results we would recommend to choose the unified methods applied on hybrid networks, ie the interconnected methods, when this is possible. But in geographically distinct locations, or when legislation prohibits system operators to share complete network data, the splitting methods are a good alternative. The speed of the CAI-schemes can be increased if we apply the idea of paragraph 4.2.3.

The next step is to continue with realistic test cases which can be up to millions of buses per network domain. In most countries, the physical transmission network is much smaller than the distribution network and a country has in general more than one distribution network. The differences between homogeneous and hybrid methods then become less significant. To solve these very large systems in reasonable amount of time, we have to adapt the methods, using Newton-Krylov methods and preconditioning techniques [23], for a parallel or GPU environment. Then, the MFS-hybrid method gets an advantage when multiple distribution networks are connected to one transmission network as it is a domain-decomposition approach: multiple distribution networks can run on parallel cores. Doing new simulations using these speed-up techniques on realistically sized networks, should give a better idea which method is most favorable to solve the integrated power flow problem.

References

[1] v. d. S. L. Schavemaker P., "Introduction to Power System Analysis," in *Electrical Power System Essentials*, ch. 1, Sussex, United Kingdom: John Wiley & Sons, Inc., 2008.

[2] Bryan Palmintier, Elaine Hale, Timothy M. Hansen, Wesley Jones, David Biagioni, Kyri Baker, Hongyu Wu, Julieta Giraldez, Harry Sorensen, Monte Lunacek, Noel Merket, Jennie Jorgenson, and Bri-Mathias Hodge, National Renewable Energy Laboratory, "Final Technical Report: Integrated DistributionTransmission Analysis for Very High Penetration Solar PV," 2016.

[3] W. H. Kersting, "The whys of distribution system analysis. Requirements for a power-flow study," *IEEE Industry Applications Magazine*, no. July, pp. 59–65, 2011.

[4] P. Schavemaker and L. van der Sluis, "Energy Management Systems," in *Electrical Power System Essentials*, ch. 6, Sussex, United Kingdom: John Wiley & Sons, Inc., 2008.

[5] P. A. N. Garcia, J. L. R. Pereira, S. Carneiro, and V. M. Da Costa, "Three-phase power flow calculations using the current injection method," *IEEE Transactions on Power Systems*, vol. 15, no. 2, pp. 508–514, 2000.

[6] M. Abdel-akher, K. M. Nor, A. Halim, and A. Rashid, "Improved Three-Phase Power-Flow Methods Using Sequence Components," vol. 20, no. 3, pp. 1389–1397, 2005.

[7] J. H. Teng and C. Y. Chang, "A novel and fast three-phase load flow for unbalanced radial distribution systems," *IEEE Transactions on Power Systems*, vol. 17, no. 4, pp. 1238–1244, 2002.

[8] T.-H. Chen, M.-S. Chen, K.-J. Hwang, P. Kotas, and E. Chebli, "Distribution system power flow analysis-a rigid approach," *IEEE Transactions on Power Delivery*, vol. 6, no. 3, pp. 1146–1152, 1991.

[9] J. Teng, "Modelling distributed generations in three-phase distribution load flow," *Generation, Transmission & Distribution, IET*, vol. 2, no. 3, pp. 330–340, 2008.

[10] H. E. Farag, E. El-Saadany, R. El Shatshat, and A. Zidan, "A generalized power flow analysis for distribution systems with high penetration of distributed generation," *Electric Power Systems Research*, vol. 81, pp. 1499–1506, jul 2011.

[11] S. M. Moghaddas-Tafreshi and E. Mashhour, "Distributed generation modeling for power flow studies and a three-phase unbalanced power flow solution for radial distribution systems considering distributed generation," *Electric Power Systems Research*, vol. 79, pp. 680–686, apr 2009.

[12] H. M. H. Eminoglu U., "The MeridiDistribution Systems Forward/Backward Sweepbased Power Flow Algorithms: A Review and Comparison Study," *Electric Power Components and Systems*, dec 2008.

[13] G. Krishnamoorthy and A. Dubey, "A framework to analyze interactions between transmission and distribution systems," in *2018 IEEE Power Energy Society General Meeting (PESGM)*, pp. 1–5, 2018.

[14] G. N. Taranto and J. M. Marinho, "A Hybrid Three-Phase Single-Phase Power Flow Formulation," *IEEE Transactions on Power Systems*, vol. 23, no. 3, pp. 1063–1070, 2008.

[15] H. Sun, S. Member, Q. Guo, S. Member, B. Zhang, and Y. Guo, "Master – Slave-Splitting Based Distributed Global Power Flow Method for Integrated Transmission and Distribution Analysis," vol. 6, no. 3, pp. 1484–1492, 2015.

[16] R. D. Zimmerman, C. E. Murillo-Sánchez, and R. J. Thomas, "MATPOWER: Steady-state operations, planning, and analysis tools for power systems research and education," *IEEE Transactions on Power Systems*, vol. 26, no. 1, pp. 12–19, 2011.

[17] W. H. Kersting, *Distribution System Modeling and Analysis, Third edition*. Las Cruces, New Mexico: CRC Press Taylor & Francis Group LLC, 3 ed., 2012.

[18] M. Bazrafshan and N. Gatsis, "Comprehensive modeling of three-phase distribution systems via the bus admittance matrix," *IEEE Transactions on Power Systems*, vol. 33, no. 2, pp. 2015–2029, 2018.

[19] H. Sun and B. Zhang, "Distributed Power Flow Calculation for Whole Networks Including Transmission and Distribution," pp. 1–6, 2008.

[20] H. B. Sun and B. M. Zhang, "Global state estimation for whole transmission and distribution networks," vol. 74, pp. 187–195, 2005.

[21] H. Sun, D. Nikovski, T. Ohno, T. Takano, and Y. Kojima, "A fast and robust load flow method for distribution systems with distributed generations," *Energy Procedia*, vol. 12, pp. 236–244, 2011.

[22] K. P. Schneider, B. A. Mather, B. C. Pal, C. W. Ten, G. J. Shirek, H. Zhu, J. C. Fuller, J. L. Pereira, L. F. Ochoa, L. R. De Araujo, R. C. Dugan, S. Matthias, S. Paudyal, T. E. McDermott, and W. Kersting, "Analytic Considerations and Design Basis for the IEEE Distribution Test Feeders," *IEEE Transactions on Power Systems*, vol. 33, no. 3, pp. 3181–3188, 2018.

[23] R. Idema, G. Papaefthymiou, D. Lahaye, C. Vuik, and L. van der Sluis, "Towards faster solution of large power flow problems," *IEEE Transactions on Power Systems*, vol. 28, pp. 4918–4925, Nov 2013.